ELSEVIER

Applied Surface Science 162–163 (2000) 227–232

applied surface science

www.elsevier.nl/locate/apsusc

Calculation of scanning inelastic tunneling profiles of adsorbates: acetylene on Cu(100)

N. Mingo *, K. Makoshi

Faculty of Science, Himeji Institute of Technology, Kamigori, Ako-gun, Hyogo 678-1297, Japan

Abstract

Several questions recently posed by Inelastic Electron Scanning Tunneling Spectroscopy (STM-IETS) experiments are clarified. First, the method of calculating inelastic currents as a function of the tip's position and the bias is shown, as well as how to relate the currents to experimental results. We apply the method to calculate the rotation rate profile of the acetylene molecule on Cu(100) as a function of the tip's displacement. The fraction of electrons inelastically scattered by the different vibrational modes of the molecule is calculated also as a function of the bias, in a range of several volts. The results of the calculation explain why the C–H bending modes were not detected in STM-IETS experiments.

PACS: 73.40.Gk; 82.65.Pa; 61.16.Ch; 68.35.Ja
Keywords: STM-IETS; Inelastic current; C–H bending mode

Several recent experiments [1–4] have proven the feasibility of measuring inelastic tunneling currents with spatial resolution using the Scanning Tunneling Microscope (STM). First, Inelastic Electron Scanning Tunneling Spectroscopy (STM-IETS) has been achieved by Stipe et al. [1,2]. Also, 'inelastic tunneling induced adsorbate manipulation' (ITM) has been reported in Refs. [3,4]. On one hand, STM-IETS can measure the inelastic tunneling fractions due to each vibrational mode of the molecule. Its limitations are some lack of sensitivity to detect weaker modes, and its inability to detect the inelastic fractions at energies other than the vibrational mode energy (when the inelastic channel opens). On the other hand, the ITM is able to report induced events due to modes that are not observed in STM-IETS, and it also can be performed for a continuum range of biases. However, ITM cannot separate the contributions of different vibrational modes. Thus, the two experimental procedures complement each other, being able to provide very useful information regarding the inelastic tunneling currents. One important concept for these experiments is that of 'inelastic profile' [5], i.e. a plot of the inelastic fraction of tunneling electrons as a function of the tip position. One example has been given in Ref. [3] by ITM, where the authors plotted the rate of flips (flips per tunneling electron) of an acetylene molecule between two equivalent adsorption orientations, as a function of the tip's displacement. Such a 'rotation rate profile' can be

* Corresponding author. Fax: +81-7915-8-0151.
E-mail address: natalio@sci.himeji-tech.ac.jp (N. Mingo).

0169-4332/00/$ - see front matter
PII: S0169-4332(00)00196-3

considered roughly proportional to the fraction of electrons inelastically scattered by the C–H stretching mode [3].

After the opening of such new experimental possibilities, some fundamental questions have arisen. The main point is, 'how to study theoretically the inelastic current problem with spatial resolution'. The existence of several vibrational modes of the adsorbate also complicates the problem [5]. Some works have dealt with the inelastic tunneling problem in different ways, however, to our knowledge the tip's position dependence of the current has never been studied. Ref. [6] is a very clear approach to the physics of the problem, in a 'one resonance + one mode' model. Presence of several orbitals in the inelastic interaction has been addressed in Ref. [7]. Ref. [8] also considers a 'one orbital' inelastic coupling model, which is not appropriate in the case of complicated molecular adsorbates like the one treated here.

Using an adequate calculational method, we can try to answer the particular questions posed by the experiments: 1 — prediction of inelastic profiles, and 2 — explanation of the relative intensity of the different modes in IETS. In the case of acetylene on Cu(100), the first question consists in predicting the inelastic profile of the molecule and comparing it with the experimental rotation rate profile. The second question is rephrased as: 'Why are the C–H bending modes not visible in STM-IETS?' [1,2]. In what follows we explain the procedure to obtain elastic and inelastic currents in a unified multiorbital approach, and then apply it to clarifying these particular questions posed by the experiment.

We have developed a many-orbital formalism to describe the inelastic tunneling currents [5]. The complete Hamiltonian is:

$$H = \sum_k E_k \hat{C}_k^\dagger \hat{C}_k + \sum_\mu \Omega_\mu \hat{V}_\mu^\dagger \hat{V}_\mu + \sum_\mu \left(\hat{V}_\mu^\dagger + \hat{V}_\mu\right) \sum_{ij} \xi_{ij}^{(\mu)} \hat{c}_i^\dagger \hat{c}_j, \quad (1)$$

$$\xi_{ij}^{(\mu)} = \left.\frac{\partial H_{ij}}{\partial \boldsymbol{R}^{(\mu)}}\right|_{\boldsymbol{R}=\boldsymbol{R}_0} \Delta R^{(\mu)}, \Delta R = \left(2m^* \Omega\right)^{-1/2} \hbar. \quad (2)$$

A localized orbital basis is used for the electrons (small cs) in the electron-vibration (e-vibr.) coupling part of the Hamiltonian. Ω is the energy of the vibrational mode. It constitutes a 'many orbital + many modes' generalization of the Hamiltonian in Ref. [6].

In Ref. [5], we showed how to obtain the different elastic and inelastic contributions to the current from Hamiltonian (1). Let us denote the different vibrational states of the molecule by arrays $\{n,m,l,\ldots\}$, where $n,m,l,\ldots$ are the number of excited levels inthe 1st, 2nd, 3rd, ... vibrational modes of the molecule. The total current is $I = \sum_{n,m,l,\ldots} I_{n,m,l,\ldots}$, where each of the contributions accounts for the electrons that excite the molecule up to the vibrational state defined by its indexes. Thus, $I_{000\ldots}$ is the elastic current, i.e. number of elastically scattered electrons per unit time. Similarly, I_{nml}/I_{000} means the fraction of electrons that are able to excite the molecule to the nth level of its first vibrational mode, mth of the second mode, and lth level of the third vibrational mode considered. Ours is an independent electron approach, in the line of Ref. [9], therefore valid if the 'coherent excitation' [9] mechanism is applicable (which is the case [3]).

The problem can be reformulated in simple scattering terms [5], where the total system is represented by a series of equivalent systems coupled by inelastic matrices. Recasting the general expression given in Ref. [5] for the conductances:

$$\sigma_{mn\ldots} = \frac{8e}{h} Tr\left[T_t \rho_t T_t^\dagger G^{\{0\ldots\}\{mn\ldots\}} \times T_s \rho_s T_s^\dagger G^{\{mn\ldots.\}\{0\ldots\}}\right] \quad (3)$$

The inelastic coupling is included in the Green function G of the equivalent system described in Ref. [5]. $T_{t(s)} \rho T_{t(s)}^\dagger$ in Eq. (3) correspond to the imaginary part of the one electron self-energy functions projected on the molecule and its surface neighbours, from the side of the tip or the sample. The inelastic currents at zero temperature can be obtained as:

$$I_{mn\ldots} = \int_{E_F}^{E_F + eV} \sigma_{mn\ldots}(E) \times \theta(E - m\Omega_m - n\Omega_n - \ldots)\, dE \quad (4)$$

Six modes are considered in this paper: C–H stretch, C–C stretch, C–H scissor, C–H wag, C–H twist and molecule–metal stretch [3]. We calculate the six inelastic conductances corresponding to the excitation of one level of each of the modes, namely σ_{100000}, σ_{010000}, etc.

The geometry of the molecule is taken from Ref. [10] ($d_{c-c} = 1.4$ Å, $d_{C-H} = 1$ Å, $d_{C\text{-metal}} = 1.65$ Å, $\phi_{C-C-H} = 116°$). To obtain the electronic structure of the sample we have followed the way described in Ref. [11]. The LCAO Hamiltonian is set, using the hopping matrix elements parametrized by Harrison [12]. They are rotated according to the usual Slater–Koster procedure [12]. As in Ref. [11], the diagonal matrix elements are taken so as to obtain the orbital levels described in Ref. [13]. A Green function technique [14] has been used to project the electronic structure of the semi-infinite metal onto the Cu(100) surface atoms. Then, the molecule is coupled to the Cu(100) surface. In the parallel direction, a periodical 3×3 surface cell has been used. Self-consistency has been taken into account by allowing a charge transfer to the molecule, as calculated in Ref. [10].

The tip has been modeled in the simplest possible way, in order not to introduce any effects other than the sample properties. Therefore, a tip apex with s-orbital symmetry has been considered. The tip's Green function onto the apex has been chosen as a constant imaginary quantity, so that the LDOS is constant in the energy range. An exponential dependence has been assumed for the tip–sample hopping matrix elements. The exponent for the tip-copper

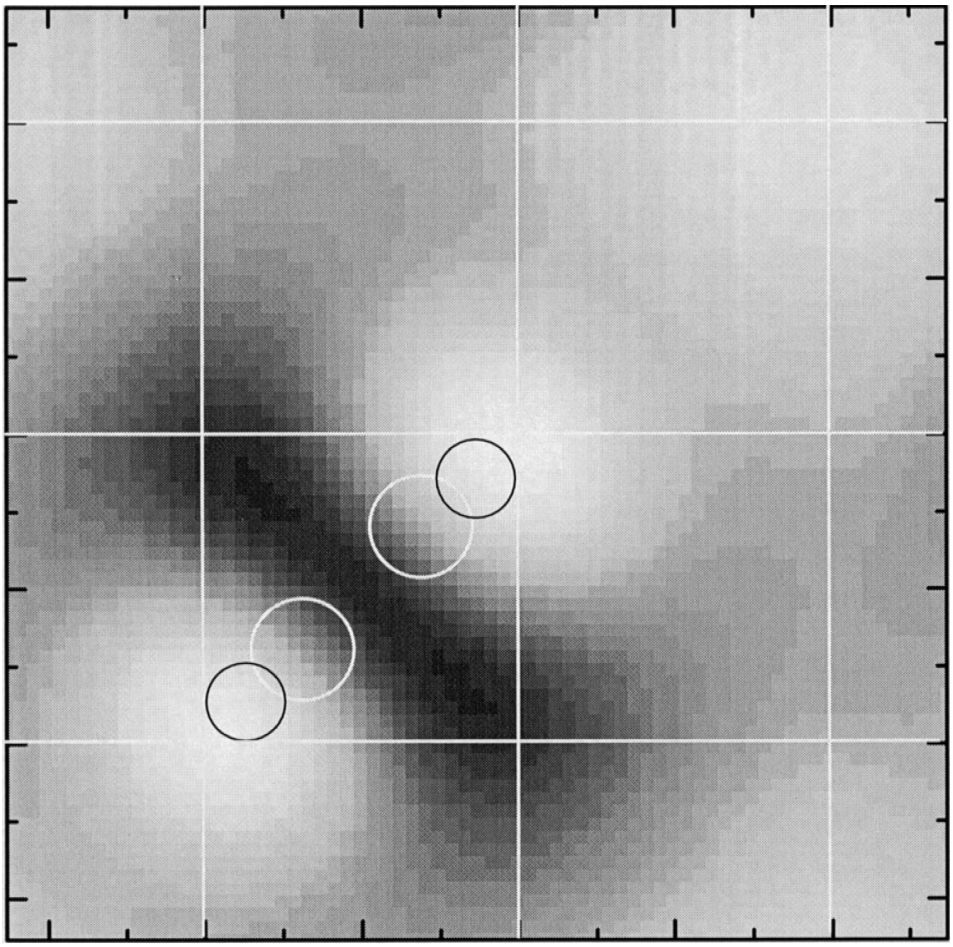

Fig. 1. Calculated constant conductance STM image of the acetylene molecule on Cu(100). The conductance is calculated in the low bias limit, $V \to 0$. The white lines indicate the surface net, and the circles mark the positions of molecule's atoms.

elements is such that the conductance vs. separation dependence agrees with the potential barrier of the metal surface. Exponents for the hopping elements between the tip and the adsorbate atoms are obtained from the Slater orbitals given in Ref. [15].

First, the elastic image of the acetylene molecule has been calculated. A dumbbell shape like the one reported in Refs. [1–3] is obtained. Fig. 1 shows the image at the 0 bias limit, for an initial tip surface separation of 7 Å. This is the separation we have used to calculate the inelastic profiles. The maximum corrugation is 0.2 Å. The position of the atoms is also shown.

Now, by using the formalism exposed above, we are able to calculate the inelastic conductances for any voltage and tip's position, in relation with two kinds of experimental measurements: (1) the direct measurement of the inelastic fraction for different modes, by IETS, and (2) the 'rotation rate' inelastic profiles, by ITM.

Let us first study the ITM profiles. The C–H stretch calculated profile dominates over all the other modes, in agreement with the experimental results. The experimental rotation rate profiles (Fig. 2 of Ref. [3]) can then be compared with the calculation for $\sigma_{\mathrm{C-Hstr.}}/\sigma_{\mathrm{elast.}}$ (Fig. 2a). The profiles have been calculated keeping the tip 7 Å over the surface atoms, starting at the center of the molecule and displacing it laterally in a range of 5 Å, following two perpendicular lines: along the molecule's axis, and perpendicular to it. The profile calculated along the axis of the molecule is higher that the one on the perpendicular, in agreement with the experiment. When the tip is laterally displaced 5 Å from the center, the calculated inelastic fraction decreases by two orders of magnitude, also in agreement with the experimental profile. The slight bump shape near the center of the molecule is due to a sharp decrease of the elastic conductance (Fig. 1). This feature is more pronounced in the experiment, and can be attributed to a higher experimental corrugation. The calculated value of $\sigma_{\mathrm{C-Hstr.}}/\sigma_{\mathrm{elast.}}$ is about 20% (about 15% of the total conductance). The fractions experimentally measured by STM-IETS are very much tip-dependent, and oscillate between 6% and 12%, being of the same order of magnitude as our result. Calculated profiles for other modes are shown in Fig. 2b, for the

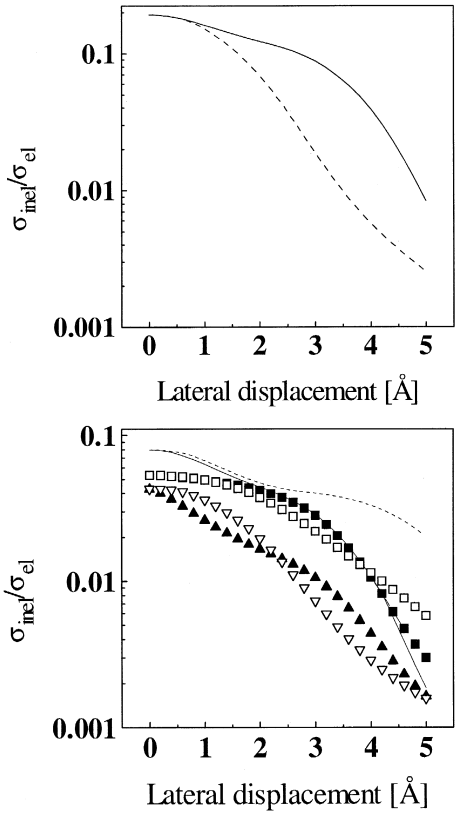

Fig. 2. The inelastic fraction of scattered electrons due to each of the vibrational modes is plotted as a function of the tip's lateral displacement, for electrons with $E = E_{\mathrm{F}}^{\mathrm{sample}}$. The 0 displacement corresponds to the tip located above the center of the molecule. Solid lines and full symbols: profile along the axis of the molecule. Dotted lines and hollow symbols: profile along the line perpendicular to the molecule's axis. Upper: C–H stretch. Lower: lines: C–C stretch; squares: C–H scissor + waging; triangles: C–H twist.

low voltage limit. Near the center of the molecule, the C–C stretching mode's inelastic fraction is 0.3 times that of the C–H stretch. This is an overestimation, being the real ratio smaller, since a 0.3 would in principle allow the STM-IETS detection of the C–C mode. A more refined Hamiltonian going beyond Harrison's matrix elements might give a smaller ratio. Nevertheless, one would not expect a significant difference regarding the order of magnitude.

We also show the inelastic profile for the in-plane H–C bending modes (the sum of both contributions is shown, to make the figure clearer), and the off-plane bending modes. All of them are much smaller than the C–H stretch for low bias and the tip over the center of the molecule. The along-axis profile

(solid lines) is always higher for the C–H stretch (Fig. 2a) than for the other modes (Fig. 2b). The perpendicular-to-axis profile (dotted lines) is also bigger for the C–H stretch near the center of the molecule, but the C–C mode becomes stronger when the tip is laterally displaced further than 2.5 Å. The same takes place for the 'in-plane' bending modes when the displacement is larger than 2.8 Å. Whether or not these modes will begin to determine the shape of the profile near these distances depends on the mechanical coupling of each of the modes to the rotation, being different in each case. Nevertheless, it could be conjectured the possible influence of the C–C and in-plane modes in the rotation rate profile over the perpendicular-axis, raising the curve for larger tip displacements. This could explain the slightly higher profile of the experimental points with respect to the calculated 'perpendicular-axis' curve when the tip is displaced more than 2 Å. We would suggest to measure experimentally the rotation rate profiles at a bias lower than the C–H stretch energy in order to clarify this point.

The second main result of this paper is related to the STM-IETS measurements. The experimental STM-IETS [1,2] performed with the tip above the center of the molecule reported an unobservability of any modes other than the C–H stretch, the reason for it remaining as a fundamental question. In order to clarify this point, we have calculated the inelastic conductance fractions for the different vibrational modes, locating the tip over the center of the molecule, for a bias range of several volts in both polarities. Results, shown in Fig. 3, display a striking difference regarding the qualitative behavior of the C–H and C–C stretching modes, compared to the C–H bending modes. While the C–H and C–C stretching inelastic conductance fractions remain quite constant in the whole range of energies, the bending modes present a much more abrupt variation. The inelastic coupling matrix elements calculated for the bending modes are similar in order of magnitude to those for the C–H stretch. Therefore, in principle one could expect their interaction with electrons to be comparable to the latter. In fact, this is the case if the voltage is increased several volts, however a sharp decrease of their inelastic conductances happens for energies closer to the Fermi level

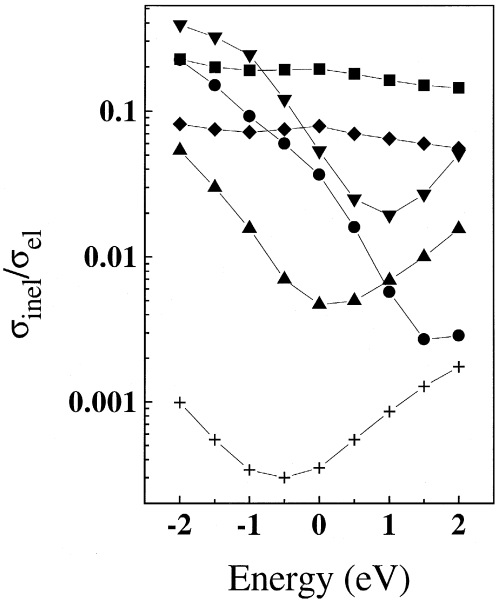

Fig. 3. Dependence of the inelastic conductance for the different modes as a function of the electron's energy. The tip is located over the center of the molecule. The inelastic conductance has been normalized by the elastic one at the same energy. The elastic conductance for this tip's position is almost constant along the energy range, changing just by about a factor of 2. Square: C–H stretch; diamond: C–C stretch; down triangle: C–H out of plane bending; up triangle: C–H wag; circle: C–H scissor; cross: molecule–metal stretch.

of the sample. The explanation for this difference of the behavior between the bending and stretching modes has to do with their different interaction with the molecular levels, regarding the relative signs of the electron-vibration coupling elements, and is related to the 'many-orbital' character of the coupling (details will be published elsewhere). Since the bending modes' energy is in all cases smaller than 0.2 eV, the results shown in Fig. 3 imply that they are not detectable by STM-IETS. However, their inelastic cross-section becomes bigger for energies several eV from the Fermi level. Thus, for high biases, they are expected to contribute to the inelastic scattering in a larger extent. This could affect the qualitative shape of the rotation rate profile with respect to lower biases too, in case the mechanical coupling of the bending modes to the rotation is comparable to that of the stretching mode.

The non-detectability of the bending modes for this system does not exclude the possibility that they

could be detected for acetylene on other metals. Although the electronic structure is expected to be similar, the relative position of the molecular orbital energy levels with respect to the Fermi level can change depending on the substrate. This would result in a different location of the minima in Fig. 3 for such a system, and a possible higher inelastic cross-section of some bending modes near the Fermi level.

We have shown how the inelastic profiles of adsorbed molecules can be calculated and compared with those experimentally reported. The calculated inelastic profile for the acetylene molecule on Cu(100) agrees well with the experimental 'rotation rate profile'. Calculated profiles for modes other than the C–H stretch are also shown. Experimental rotation rate profiles taken at biases smaller than the C–H stretch energy would help in determining the relative coupling of those modes to the rotation. We have reported a qualitatively different behavior between the bending modes and the C–H and C–C stretching modes inelastic fraction, as a function of the energy. This answers the question on the non-detectability of the C–H bending modes while doing IETS, raised by the experiments. The ability to calculate inelastic currents with spatial resolution as well as bias dependence has been shown for the first time. We hope it will stimulate experiments measuring inelastic profiles of adsorbates with spatial and bias resolution in STM.

Acknowledgements

We acknowledge M. Rose, M. Salmeron, R. Perez and F. Flores for helpful comments. N.M. acknowledges a fellowship from the EU.

References

[1] B.C. Stipe, M.A. Rezaei, W. Ho, Science 280 (1998) 1732, and references therein.
[2] B.C. Stipe, M.A. Rezaei, W. Ho, Phys. Rev. Lett. 82 (1999) 1724, and references therein.
[3] B.C. Stipe, M.A. Rezaei, W. Ho, Phys. Rev. Lett. 81 (1998) 1263.
[4] L. Bartels, G. Meyer, K.-H. Rieder, D. Velic, E. Knoesel, A. Hotzel, M. Wolf, G. Ertl, Phys. Rev. Lett. 80 (1998) 2004.
[5] N. Mingo, K. Makoshi, Surf. Sci. 438 (1999) 261–270.
[6] B.N.J. Persson, A. Baratoff, Phys. Rev. Lett. 59 (1987) 339.
[7] M.A. Gata, P.R. Antoniewicz, Phys. Rev. B 47 (1993) 13797.
[8] K. Stokbro, B.Y. Hu, C. Thirstrup, X.C. Xie, Phys. Rev. B 58 (1998) 8038.
[9] P. Salam, M. Persson, R.E. Palmer, Phys. Rev. B 49 (1994) 10655.
[10] S. Hengrasmee, J.B. Peel, Surf. Sci. 184 (1987) 434.
[11] B. Hellsing, Surf. Sci. 282 (1993) 216.
[12] W.A. Harrison, Electronic Structure and the Properties of Solids, Freeman, New York, 1980.
[13] D.M. Hoffman, R. Hoffmann, R. Fisel, J. Am. Chem. Soc. 104 (1982) 3858.
[14] F. Guinea, C. Tejedor, F. Flores, E. Louis, Phys. Rev. B 28 (1983) 4397.
[15] J. Silvestre, R. Hoffmann, Langmuir 1 (6) (1985) 621.